

System Level Exergy Assessment of Strategies Deployed for SOFC Stack Temperature Regulation and Thermal Gradient Reduction

Shi Tang¹, Amirpiran Amiri^{*2}, Moses O. Tadé³

¹Hubei Key Laboratory of Mechanical Transmission and Manufacturing Engineering, Wuhan University of Science and Technology, Wuhan, 430081, PRC

²European Bioenergy Research Institute (EBRI), School of Engineering and Applied Science, Aston University, Birmingham, B4 7ET, United Kingdom

³Discipline of Chemical Engineering, Curtin University, Kent Street, Bentley, WA 6102, Australia

*Corresponding Author: a.p.amiri@aston.ac.uk

Abstract

Several operational strategies for Solid Oxide Fuel Cell (SOFC) temperature regulation and temperature gradient minimization at cell scale have previously been assessed by the authors (Amiri et al., Ind. Eng. Chem. Res., 2016). The application of such strategies at system scale, however, requires a numerical linkage between the cell and system performance metrics allowing simultaneous evaluation of the dominant process interactions. The objective of this study is to analytically examine the effectiveness and applicability of the mentioned thermal management methods at system scale. To achieve this, a system level exergy analysis is presented by using a modelling platform in which a detailed 4-cell short stack module and the Balance-of-Plant (BoP) are integrated. Linkage between the system performance metrics and the stack internal temperature gradient is specifically emphasized. For this, the exergy intensive points (unit operations) are identified throughout the plant. Subsequently, the effective strategies that had been employed for the cell level thermal management proposed in our previous work (Amiri et al., Ind. Eng. Chem. Res., 2016) are examined at the system level capturing the effects on the state of BoP exergy intensive components. Moreover, fuel design is proposed and evaluated as a potential thermal management strategy. Combination of variety of measures including the exergy destruction rates, the electrical and thermal efficiencies, and the stack internal temperature gradient provides a comprehensive set of data contributing to the SOFC system thermal management.

Introduction

The role of SOFC technology in addressing the current and future challenges relevant to the world energy demand is crucial. SOFCs offer an efficient and environmentally friendly process to convert chemical energy to electrical energy. The wide spectrum of applications,

1 fuel diversity, and high efficiency are typical examples of SOFC technology attractions.
2 However, SOFC system commercialization has been experiencing serious bottlenecks
3 associated with hardware efficiency and durability in addition to sub-optimal operational
4 techniques. In order to fundamentally confront these drawbacks, tremendous efforts have been
5 devoted to this area, at various scales of SOFC system, i.e., micro-, meso-, and macro-scale,
6 by researchers worldwide.¹ However, the knowledge gaps are still significant demanding
7 further insightful research and development endeavours.

8

9 Technical malfunctions such as cell degradation that can cause the unit failure, spare part
10 costs, and reliability risks, are serious challenges that currently decelerate the SOFC
11 commercialization. While fuel cell degradation is mainly attributed to the materials and
12 catalyst physicochemical properties and fuel contaminations,^{2,3} it is also strongly linked to the
13 thermal instability and stress.^{4,5} The latter is particularly important in SOFC case operating at
14 elevated temperatures (700-900°C) with a high temperature gradients across stack dimensions.
15 Thermal management of SOFC operation is necessary to enhance the stack durability and
16 improve the entire system efficiency leading to an economic viability. Thermal management
17 concept includes not only reduction of thermal stresses inside the SOFC stack by improving
18 thermal homogeneity, but also integration of the heat-sinks and heat-sources throughout the
19 BoP. In this view, thermal management analysis should account for the mentioned aspects at
20 deferent scales targeting sufficient details. To address this, high-fidelity numerical tools that
21 encompass capabilities to capture the multi-scale-multi-physics nature of the fuel cell system
22 are required.

23

24 A wide range of thermal analysis modelling studies have been conducted to identify the
25 challenges and opportunities for improving the SOFC performance at cell scale. Previous
26 studies have demonstrated a substantial temperature gradient inside the planar SOFC,
27 typically up to 10 K/cm for instance.^{6,7} Minimization of the temperature gradient is of crucial
28 importance to effectively control internal thermal stresses and degradation rate.⁸ Through
29 numerical studies of cell thermal performance it has been proven that both cell design
30 (geometry) and operational factors contribute to temperature gradient. For given SOFC
31 geometry design, the process variables such as operating temperature and voltage, fuel and air
32 flow rates, etc., are typical dominant variables that can be tuned to attain a thermally efficient
33 operation at cell scale.⁹⁻¹² However, the system-wide impacts of the manipulated variables
34 must not be compromised. For instance, while higher air flow rate leads to a lower temperature

1 gradient, it can controversially increase the operation cost due to higher blower power and
2 sizing issues. Riensche et al.¹³ have shown that the plant-wide operation cost can reduce by
3 20% by allowing higher temperature increase across the cell, 150 K instead of 100 K. Authors
4 have previously investigated the operating strategies that result in efficient control of thermal
5 inhomogeneity inside SOFC without causing major efficiency/cost consequences.¹⁴ In the
6 mentioned work three operational variations, including the surplus air flowrates, the input
7 gases temperature difference, and the oxygen concentration in cathode gases, have been
8 proposed and extensively analyzed to demonstrate their impacts of temperature gradient
9 reduction. However, these operating approaches must be assessed at the system level where a
10 shortcoming exists in terms of understanding the interaction between system efficiency and
11 stack function homogeneity, performance loss mechanisms, and overpotentials, etc. At the
12 system/plant scale the optimum energy generation and utilization are commonly targeted. In
13 this view, exergy analysis is a technically informative approach for evaluation and
14 optimization of plant convertible energy and energy losses. For a complex thermodynamic
15 system, the exergy analysis allows for the local energy destruction calculations associated
16 with the sub-processes in the system that are necessary information needed for entire plant
17 optimization.¹⁵⁻¹⁷

18
19 The SOFC efficiency maximization based on the exergy evaluation has been investigated in
20 the literature without considering the BoP compartments influences.¹⁸ Compared to the isolated
21 SOFC cell performance, the electrochemical behaviour of SOFC stack embedded in a system
22 can be different and more complicated due to the BoP units interactions, indicating the
23 importance of system features that have not sufficiently been studied in the mentioned
24 literature. Various SOFC plant flowsheets, including different co-generation plants, have been
25 considered to demonstrate the system configuration as a promising option for system efficiency
26 enhancement.¹⁹⁻²¹ Additionally, efficiency improvement via operating parameters tuning, such
27 as anode off-gas recycle ratio, and operation strategies, such as internal reforming, etc., have
28 been studied^{19,22-26} using exergy concept. The drawback in these studies is the stack details that
29 have been ignored or simplified while deployment of the proposed methods may affect the
30 stack operation uniformity and stability.²⁷ Calise et al.²⁶ conducted an exergy analysis for a
31 SOFC plant, considering variables distributions in the stacking direction of a tubular SOFC,
32 while it cannot represent the planar SOFC behaviour due to geometry and the distributed
33 variables differences. Accordingly, this work – compared to the literature as shown in Table 1
34 – presents a state-of-the-art contribution to the SOFC stack and system thermal management

1 using a plant scale exergy analysis. This study illustrates the mutual interaction between the
2 stack and system performances. The investigation demonstrates the extent to which various
3 operational strategies can be effective to improve the stack thermal performance and system
4 exergy dissipation.

5
6 **Table 1:** Comparison of a number of recent SOFC exergy studies.

7 **SOFC system simulation platform**

8 The process exergy analysis highly relies on the plant data including streams mass and energy
9 data and mixtures physicochemical properties. A SOFC simulation platform developed by
10 authors^{28,29} was used in this work to achieve the mentioned raw data. The simulator has already
11 been validated against a real-life SOFC system rig approving its capability of a multi-scale
12 performances capturing of the SOFC system.³⁰ The platform capability and fidelity for
13 estimating the BoP mass and energy balances and the stack internal profiles have been
14 demonstrated and validated in our previous research.²⁹ The simulated process flowsheet was
15 selected to be rather comprehensive encompassing the main sub-processes of a SOFC plant
16 including fuel conditioning, power generation through electrochemical process, depleted-fuel
17 combustion and the heat recovery units that are the most likely elements of the system for the
18 commercialization in short-term³¹. The analysis outcome relevant to each operation units may
19 be generalized when the process configuration changes. This is because the fundamental
20 equations used still apply, in spite of change in unit location and inputs. Therefore, the
21 presented modelling framework is capable enough to be used for various fuel cell system
22 layouts.

24 **Energy and exergy analysis fundamentals**

25 Given the process flowsheet data, the energy and exergy analysis for SOFC system were carried
26 out based on the fundamental equations as follows. Energy for each stream was calculated based
27 on the enthalpy correlation (Equation 1).

$$29 \quad E = \sum \dot{m}C_p(T - T_0) \quad (1)$$

30 The net electrical efficiency of system based on energy analysis was calculated as by using
31 Equation 2,³²

$$32 \quad \eta_{el}^{en} = \frac{P_{net}}{(\dot{m}.LHV)_{fuel}} \quad (2)$$

1 While the fresh air blower is the main power consumption module in the system due partly to
 2 the high air-to-fuel flowrate ratio and long fluid flow line downstream, the anode off-gas recycle
 3 line pressure drop might be effective on the overall system performance. The pressure drop in
 4 recycle line may typically be ~80 mbar.¹⁹ The simulation platform allows the pressure drop
 5 consideration in individual components throughout the plant. Since hydrodynamics calculations
 6 were out of this work scope, the units' pressure drops were assumed to be constant values
 7 published in literature.^{19,33} An anode recycle blower was considered to compensate the anode
 8 recycle line pressure drop, as shown in the process flow diagram, Figure 1. The blower duty
 9 would be estimated by simulator based on the total pressure drop in the, pre-reformer and stack
 10 anode channels. The relevant power consumption term appears in Equation 3 slightly affecting
 11 performance metrics. The isentropic efficiency for the blowers was assumed to be 60% .³⁴

$$12 \quad P_{net} = (UI)_{stack} - P_{bl}^{air} - P_{bl}^{recycle} \quad (3)$$

13 For the SOFC system in this study, the high grade exhaust gas temperature was around 400 K
 14 that could be utilised for heating purposes.³⁵ For evaluation of available thermal energy (E_{th}) in
 15 the system, the enthalpy of the system exhaust gas was calculated. The portion of the exhaust
 16 heat that can be recovered can vary from ~38% to ~70% depending on the recovery process
 17 type and design.^{19, 36,37} For comparison purpose the heat recovery ratio, ε , was assumed to be
 18 60% in the current work. Accordingly, the thermal efficiency of the system can be estimated
 19 using Equation 5:

$$20 \quad \eta_{th}^{en} = \frac{\varepsilon E_{th}}{(\dot{m}.LHV)_{fuel,in}} = \frac{\varepsilon E_{ef}}{(\dot{m}.LHV)_{fuel,in}} \quad (4)$$

21 For the exergy analysis, the exergy for each material stream was estimated based on the physical
 22 (Ex^{ph}) and chemical (Ex^{ch}) exergies:²³

$$23 \quad (Ex)_m = Ex^{ch} + Ex^{ph} \quad (5)$$

24 Chemical exergy of a material stream can be calculated by using Equation 7:^{18, 23}

$$25 \quad Ex^{ch} = \sum_i \dot{m}_i Ex_i^0 + RT_0 \sum_i \dot{m}_i \ln(y_i) \quad (6)$$

26 Streams physical exergy can be estimated through Equation 8:²³

$$27 \quad Ex^{ph} = \dot{m}[(h - h_0) - T_0(s - s_0)] \quad (7)$$

1 Exergy-based thermal and electrical efficiencies can be calculated using Equation 9 and 10,
 2 respectively. The thermal exergy was estimated as recoverable portion of the effluent stream
 3 physical exergy.

$$4 \quad \eta_{el}^{ex} = \frac{P_{net}}{Ex_{in}} \quad (8)$$

$$5 \quad \eta_{th}^{ex} = \frac{\varepsilon Ex_{th}}{Ex_{in}} = \frac{\varepsilon Ex_{ef}^{ph}}{Ex_{in}} \quad (9)$$

6 Accordingly, the total efficiency with respect to exergy is,

$$7 \quad \eta_{total}^{ex} = \frac{P_{net} + \varepsilon Ex_{th}}{Ex_{in}} \quad (10)$$

8 The destroyed exergy or irreversibility associated with an individual process was calculated
 9 based on the input/output exergy of the material stream, heat stream and power for the process:²³

10

$$11 \quad Ex_{ir} = \sum_{in}(Ex)_m - \sum_{out}(Ex)_m + \sum_{in}(Ex)_h - \sum_{out}(Ex)_h - \sum(Ex)_p \quad (11)$$

$$12 \quad (Ex)_h = \left(1 - \frac{T_0}{T}\right) Q \quad (12)$$

13 in which, exergy of material streams, $(Ex)_m$, was calculated based on Equation 6, 7 and 8;
 14 exergy of heat streams, $(Ex)_h$, was estimated based on Equation 13, where Q is the available
 15 heat energy at temperature T; power exergy, $(Ex)_p$, equals to the power itself.

16 Accordingly the destroyed-to-input exergies ratio can be calculated as:

$$17 \quad \mu_{ir}^{ex} = \frac{Ex_{ir}}{Ex_{in}} \quad (13)$$

18

19

20

21 **Results and discussions**

22 **Exergy intensive units**

23 The local irreversibility in process compartments/units, alternatively known as exergy
 24 destruction associated with individual BoP elements, was firstly calculated. For this target, plant
 25 simulation results were used in the exergy correlations. This allows shortlisting the exergy-
 26 intensive points of process that must be specifically focused on during the assessment of the

1 cooling strategies. The process flowsheet and simulation inputs are shown in Figure 1 and Table
2 2, respectively. The process flow diagram is a generic one that consists of major BoP units such
3 as gas blower, heat exchangers fuel burners, external reformer, etc. Since this paper aims at a
4 plant-wide exergy analysis, the system flowsheet was selected in the way that involves the
5 major BoP components that might be the bottlenecks in terms of exergy destruction. In all of
6 the simulation cases in this paper the external fuel processing was considered ensuring less than
7 0.5% (molar) of methane in reformer exhaust stream, fed into SOFC stack. Therefore, the
8 internal reformation was negligible.

9
10
11 Figure 1: Process layout for a SOFC system showing the indicative exergy results for the
12 basis case (BC) simulation including the sub-process exergy loss (rectangular boxes with
13 arrow), exergy loss to the input exergy into the system ratio (oval boxes), and system input
14 and output exergies (rectangular boxes without arrow).

15
16
17
18
19 Table 2: The model parameters for the electrochemical simulation of the
20 SOFC stack and system (BC).

21
22 Shares of system energy/exergy elements are depicted in Figure 2. The electrical output
23 percentage is associated with energy analysis is higher than that in exergy analysis. The value
24 of input fuel exergy is higher than the energy input estimated based on the LHV while
25 generated electricity is the same in both cases. The system recoverable and wasted heat
26 estimated through exergy- and energy-based analyses show substantial differences. This is
27 mainly because of destroyed exergy considerations. Figure 2 indicates how share values may
28 alter using either energy or exergy concepts as the assessment basis. The conversion of energy
29 is evaluated in the energy analysis, according to the first law of thermodynamics. For this
30 study, electrical power and heat waste construct the input energy. While in the exergy analysis,
31 based on second law of thermodynamics, a portion of the energy is destroyed and cannot be
32 converted to the work (irreversibility), leading to the entropy increase in the process,

1
2
3
4
5
6
7
8
9
10
11
12
13
14
15
16
17
18
19
20
21
22
23
24
25
26
27
28
29
30

Figure 2: The plant analysis based on the energy and exergy principles.

Parameter studies of thermal behavior

The process features at the stack and system scales were integrated. In this view, process characteristics measures including the stack temperature gradient, system efficiency, individual efficiency terms, and irreversibility values were estimated examining the promising thermal-effective scenarios. Four operational strategies including the utilization of surplus air, deployment of oxygen-enriched air, manipulation of anode exhaust recycling rate, and variation of fuel source were assessed. For all case studies, the various fuels and air with proper qualities, were assumed to be ready to be fed into the system. The gases production processes such as oxygen enrichment process, gasification, etc., were not considered. The exergy of system material streams were estimated based on Equation 5-7.

Case 1: Utilization of surplus air

The SOFC cathode is supplied with air to exploit its cooling potential and as the oxygen supply for quintessential electrochemical reaction. It is widely acknowledged that regulation of the temperature rise and the thermal gradient inside the SOFC stack can be achieved and maintained by the utilisation of an optimized flow of excess air. Careful optimisation must be conducted by considering the necessary trade-off between the mentioned advantages and the disadvantages relevant to sizing and parasitic losses. The impact of excess air deployment on system efficiency terms (thermal and electrical), total efficiency, and exergy losses have been estimated. A sensitivity analysis has been carried out for the system operating with the air flowrate ranging from 50% to 200% of \dot{m}_{basis}^{air} where \dot{m}_{basis}^{air} is the air mass flowrate of base simulation. For the sake of viability, the manipulating range was chosen to be consistent with the practical excess air ratios reported in literature.^{19, 38-39} The fuel flowrate was kept consistently unchanged in all studied cases. The impacts on the system and stack performance metrics are presented in Table 3. In addition, effects on the exergy losses at various parts of the BoP are presented in Figure 2.

Table 3: Variation of system and stack metrics with air flowrate

The results shown in Table 3 reveal that the stack average temperature and its gradient (ΔT_x)

1 are strongly affected by the air flowrate applied to the system. Temperature uniformity has
2 been remarkably enhanced at higher airflows. The observed results are in agreement with the
3 previous research outcomes.^{9, 40} The outcomes are particularly of technical importance to
4 minimize thermal stresses and also achieve homogenous reaction profiles inside stack. At the
5 system scale, however, the negative consequences are markedly worrying; further restraining
6 the deployment of this strategy. For instance, for the air flow ratio varying from 0.5 to 2.0
7 a system operating at a constant voltage, the electrical efficiency experiences significant
8 reduction, approximately 7.2%; due to the interactive cooling effect (~104 K) and the
9 electrochemical reaction rate that result in current generation drop. Moreover the higher air
10 flow, the high air blower power consumption would be imposed on the system reducing P_{net} .
11 Furthermore, thermal efficiency declines by 4.8%. In this view, the electrical efficiency is seen
12 to be more sacrificed by deployment of surplus air, compared to thermal efficiency.
13 Principally, the share of electrical efficiency in achievable total efficiency is dominant. In the
14 best case the thermal efficiency can improve the overall efficiencies by 7.6%; in this particular
15 case study. The total exergy efficiency is reduced by 12.0% due to the reduction in both current
16 generation and increased exergy losses. The part of fuel exergy that was not harnessed as
17 electrical power could not be gained as thermal energy, as the exergy losses values show.

18 The influence of exploiting surplus air on exergy intensive units is presented in Figure 3. As
19 can be seen in this figure, the exergy loss growth with excess air for exergy intensive units,
20 the total loss is mainly dominated by the boosted exergy dissipation in the air preheater due
21 to higher air flowrates. A similar, but moderated, behavior was observed in other equipment
22 such as, the after burner, fuel preheater, etc. In these units since temperature differences are
23 much lower in contrast to temperature change in the air heater, lower exergy losses are
24 observed.

25

26 Figure 3: Ratio of the exergy losses to the total exergy input for different air flow rates.

27 **Case 2: Utilisation of oxygen-enriched air**

28 The higher partial pressure of oxygen in the cathode gas can enhance the stack electrical
29 efficiency. The rational reason that explains this is the improved electrochemical reaction,
30 Nernst voltage and the reduced overpotentials.^{20,41} Grounded on this, it has been shown in our
31 previous work¹⁴ that utilization of oxygen-enriched air, instead of natural air may, to some

1 extent, compensate the negative consequences caused by surplus air exploitation in the SOFC
2 stack for cooling. However, since air treatment imposes extra process costs, the process
3 economics has also been assessed in¹⁴ to figure out the practical margins. As the last but not
4 the least step, feasibility study at plant level was conducted in this work.

5 A range of oxygen concentrations in the cathode air were examined. The performance metrics
6 for the entire system and individual plant components were calculated as presented in Table 4
7 and Figure 4. The overall system efficiency shows 1.7% growth by doubling the air oxygen
8 quality. This is due to the electrical performance enhancement up to 2.7%. However, the
9 thermal efficiency and the temperature distribution smoothness are negatively affected. Since
10 fuel utilization is increased along with the higher current generation according to Faraday's
11 Law the enhancement of the electrical performance leads to the lesser amount of unreacted
12 fuel remained in the anode exhaust that consequently generates lower combustion heat in the
13 burner. Accordingly the exhaust temperature drops causing heat quality reduction. Note that
14 the overall irreversibility slightly drops, about 1.5%, with the oxygen quality as shown in
15 Table 4. The detailed exergy results associated with the exergy-intensive units reveals that the
16 irreversibility improvement is mainly attributed to the burner unit due to the lower amount of
17 fuel being combusted compared to the BC. Furthermore, taking the air pre-heater module into
18 account, since the process stream (air) flowrate and temperature growth are kept the same in
19 all of the case studies, the minor variation of exergy loss in this unit is because of the hot
20 stream physicochemical properties variation such as its heat capacity as function of the gas
21 mixture composition.

22
23 Table 4: Simulation results for the system and stack behavior deploying various oxygen
24 concentration in cathode.

25
26 Figure 4: Ratio of the exergy losses to the total exergy input for different oxygen
27 concentrations used in cathode gas.

28 29 **Case 3: Anode off-gas recycle**

30 Anode off-gas recycle stream in the BoP is to increase the stack efficiency through improving
31 the fuel utilization and the heat and water recovery.^{19, 42} Even though the maximum overall
32 (system) fuel utilization is a sought-after target, the single-pass fuel utilization must be kept
33 limited within a safe margin to control the concentration loss and fuel starvation inside cells.
34 Optimization of the anode recycle ratio (ARR) allows to chive this target. The impact of ARR

1 variations on BoP exergy dissipation and the stack internal profiles must be considered as
2 crucial constraints or even objectives in defining the ARR optimization problem.

3
4 The estimated results for both system and stack performance against ARR alteration are
5 presented in Table 5. Moreover, Figure 5 depicts the process compartments exergy losses
6 versus ARR. It can be seen that while higher ARR improves the system efficiency, it may lead
7 to a higher degree of thermal inhomogeneity inside the stack. Even though a stack with
8 complete external fuel reformation is considered in this study, it reasonably compares with
9 the results achieved by Nikooyeh et. al.⁴³ for internal fuel reformation.

10
11
12 Table 5: Simulation results for the system thermal behaviour against ARR.

13
14
15
16 The modelling results presented in Table 5 demonstrates the substantial negative effect of
17 ARR on the interior temperature distribution increasing thermal gradient by ~30% for ARR
18 ranging from 0.1 to 0.7. In contrast, the electrical efficiency improves with the anode ARR
19 owing to the electrochemical reaction enhancement. With variation of ARR from 0.1 to 0.7,
20 electrical efficiency is improved up to 5.4% while thermal efficiency slightly reduces that is
21 mainly contributed to the lower amount of unreacted fuel left that results in lower heat grade
22 at the burner exhaust.

23
24 A reduction in irreversibility ratio, about 3.5%, is also observed for whole ranges of the ARR
25 in Table 5. The individual exergy behaviours versus the ARR are shown in Figure 5. While
26 burner exergy is highly sensitive to the ARR variations, its effect on the air preheater and
27 other BoP components is minor. This is because at higher fuel utilization at higher ARR,
28 lowering the unreacted fuel flow fed to burner. Furthermore, the anode exhaust temperature
29 is risen, moderating the temperature difference between the burner inlet and outlet. The lower
30 temperature difference and lower fuel flow, explains the declining burner exergy loss. Other
31 BoP compartments exergy loss increased with the ARR. This can be mainly ascribed to the
32 increased flowrate of the recycling stream passing through the anode mixer and pre-reformer.
33 The controversial behaviour captured for the system performance metrics and the stack
34 thermal inhomogeneity requires a trade-off between system efficiency and durability.

1
2
3
4
5
6
7
8
9
10
11
12
13
14
15
16
17
18
19
20
21
22
23
24
25
26
27
28
29
30
31
32
33

Figure 5: Effect of ARR on BoP units' exergy loss ratio.

Case 4: Fuel variation

Since SOFC has capability to be fuelled with various fuels, fuel design might provide potentials to minimize the internal gradients while system electrical and thermal requirements are met. Process analysis was furthered to examine different fuels in the operation, monitoring the system performance and stack thermal measures. The so-called "Designed Fuel" is syngas mixed with the basis fuel (Table 2 and 6). All of the studied fuel sources are shown in Table 6. The syngas composition used in this study was given in literature⁴⁴. It is actually a coal-derived syngas (LHV = 217.24 kJ/mol) and is assumed to be available to be fed into the system. Accordingly, the only fuel processing for such a feed is the WGR. For the methane rich case (BC, LHV = 724.13kJ/mol) both SR and WGR occur and reformat (stack feed) composition is very different compared to reformat achieved in syngas case. SR, due to its endothermic nature, enables to recover the exhaust heat as electricity, and hence reducing the destroyed exergy, which is not that possible in the syngas-fed system. For the sake of consistency fuel flow ratios were adjusted to ensure the same exergy input in all cases. As can be seen in Table 6, a significant electrical efficiency reduction of ~29.9% is observed for the syngas fraction varying from 0 to 1, while smoother thermal profiles are achievable. The hydrogen quality in a syngas enriched fuel is lower than basis fuel. Moreover, average operating temperature lowered due to higher gas flow and also reduced heat released from electrochemical reaction. All of these, result in the reduced current generation and electrical efficiency. The key point is that the total exergy efficiency experiences 15.2% reduction that is explainable via thermal efficiency improvement.

Table 6: Simulation results for the system thermal behaviour operating on different fuels.

The individual loss variations in BoP elements against fuel composition are illustrated in Figure 6. In contrast to Case 1, the higher fuel flowrate of simulated fuels, required to ensure the equal input exergy, does not cause an outstanding irreversibility growth, being only around 5.1%. The exergy loss is because of the increase in entropy that is a function of gas flowrate

1 and its temperature change. The exergy loss in air heater increased slightly with the increase
2 of syngas fraction. This would be the results under both effects of lower temperature
3 differences for the heat exchanging process caused by the decreased stack exhausts
4 temperature, and also the increase of the fuel flowrate. The exergy loss in the after burner
5 increases slightly as well, this could attribute to both the higher content of the un-reacted fuel
6 in stack anode exhaust and the increase of fuel flowrates.

7 The exergy dissipation for pre-reforming process, including fuel preheating and reformation,
8 declines with the syngas fraction. This is due to the exothermic nature of the syngas reforming
9 reaction, increasing the reformat temperature that subsequently leads to a lower heating duty.
10 In this case, therefore, the reduction of irreversibility due to the exothermic reaction makes up
11 the irreversibility generated by flowrates, saving exergy, in comparison to Case 1.

12 This is of interest in the systems in which thermal-to-electrical performance must be balanced
13 such as SOFC system used for residential applications. Syngas, in contrast to the BC, sounds
14 promising for achieving thermal smoothness and higher thermal-to-electrical performance
15 ratio. Note that syngas from sources rather than natural gas, such as biomass gasification, may
16 include higher contaminants. The impact of fuel contaminants on SOFC degradation is out of
17 scope of this study. For assessing the SOFC lifetime improvement, one should consider both
18 thermal malfunctions/damages and contaminant relevant degradation.

19

20 Figure 6: Ratio of the exergy loss to the total exergy input for different fuel compositions
21 used in the system.

22 **Optimization strategy**

23 For a system fed by a fixed fuel (the BC), the system efficiency variation against ΔT_x for
24 individual strategies is presented in Figure 7. The simultaneous evaluation of stack thermal
25 behavior and system efficiency reveals that there are two operation regions including the
26 system efficiency improvement region and the stack thermal improvement region. Each region
27 offers specific possibilities for trade-off between the stack and system design and operation.

28 Figure 7: System efficiency against the stack temperature gradient for individual operational
29 strategies.

30

1 Taking the limitation of the technically feasible ranges for each variable into account, the
2 scope of surplus air application was the widest among the studied approaches. Moreover, in
3 the stack thermal improvement region the surplus air application was observed to be more
4 effective approach for the temperature gradient improvement offering less negative influence
5 on the system efficiency compared to the ARR reduction method. It, however, affects the
6 system efficiency in an opposite way. Within the system efficiency improvement region the
7 total efficiency can be improved through deploying oxygen enriched-air, slightly sacrificing
8 the stack thermal homogeneity. The range of maneuver is rather limited as air enrichment is
9 not readily possible. Similar affects were observed for ARR strategy causing a relatively
10 higher ΔT_x inside the stack in contrast to the enriched-air application. Therefore, it can be
11 concluded that the excess air is the preliminary method for the stack thermal management
12 being combined with a higher ARR and enriched-air utilization for the system efficiency
13 improvement purposes. Figure 8 demonstrates the system efficiency against the stack
14 temperature gradient for the combined strategies. Each operating line shows the excess air
15 flow (ranging from 50-200% of the BC air flow) effects on the system efficiency and the stack
16 ΔT_x while the specified ARR and oxygen fraction were adjusted in the operation.

17

18 Figure 8: System exergy-based efficiency against the stack thermal gradient for coolant air
19 flowrates varying from 0.5 to 2 times of the basis air flow, combined with ARR and y_{O_2}
20 impact.

21

22

23 **Conclusion**

24 In spite of the substantial progress in fuel cell technology in the last two decades, its lifetime
25 is yet to be improved to address the commercialization requirements. In order to deal with this
26 challenge, operational techniques that result in thermally homogenous SOFC performance is
27 of high importance. In this paper, as a scaled-up modelling study, the SOFC stack thermal
28 homogeneity and system exergy were simultaneously evaluated. The focus was on the
29 investigation of four different cases including the utilization of surplus air, deployment of
30 oxygen-enriched air, manipulation of anode exhaust recycling rate, and variation of fuel
31 source. The main outcomes of this study are as follows:

- 1 • Application of surplus air is highly effective for temperature adjustment and thermal
2 uniformity on the cost of thermal and electrical efficiencies reduction and also increase
3 in exergy destruction in all of BoP compartments, the air pre-heater in particular. In
4 spite of the higher stack efficiency at smoother temperature profile, the system overall
5 efficiency shows the reduction that demonstrates the critical role of the exergy losses.
6 The optimized excess air flow should be achieved through a multi-objective
7 optimization that compromises the stack thermal homogeneity and the overall system
8 efficiency.
- 9 • Utilization of oxygen-enriched air was considered to see if it can compensate for a
10 portion of the efficiency sacrificed by using surplus normal air. The results indicated
11 that electric and thermal efficiencies increases and decreases, respectively when
12 oxygen enriched air is used. However the total improvement in net efficiency is less
13 than 3% by doubling oxygen fraction in the used air.
- 14 • It is observed that the thermal gradient is negatively affected by higher ARR while it
15 is positively effective for efficiency improvement and water management in the SOFC
16 system.
- 17 • Fuel composition adjustment is shown to be a potential methodology to successfully
18 balance thermal homogeneity and system efficiency. Moreover it has been observed
19 that this method can be used to balance the thermal and electrical efficiencies that is
20 compatible for the application of interest.
- 21 • While the trade-off between system electrical efficiency and homogeneity of stack
22 operation is usually essential, the modelling results show that simultaneous
23 enhancement in stack internal profiles and system thermal efficiency is feasible.

25 **Acknowledgements**

26 The authors acknowledge the financial supports by Hubei Provincial Natural Science Foundation of China (Grant
27 No. 2018CFB143) for this research.

1 Nomenclature

| | | |
|----|--------------------------|---|
| 2 | C_p | Specific heat ($\text{J mol}^{-1} \text{K}^{-1}$) |
| 3 | E | Energy (W) |
| 4 | E_x | Exergy (W) |
| 5 | E_x^0 | Standard chemical exergy (J mol^{-1}) |
| 6 | F | Faraday's constant ($96,485 \text{ C mol}^{-1}$) |
| 7 | h | Enthalpy (J mol^{-1}) |
| 8 | I | Current (A) |
| 9 | LHV | Lower heating value (J mol^{-1}) |
| 10 | \dot{m} | Molar flow rate (mol s^{-1}) |
| 11 | N_e | Number of electrons |
| 12 | P | Pressure (Pa) |
| 13 | P_{in}^{System} | System input power (W) |
| 14 | P_{net} | Net power (W) |
| 15 | P_{bl} | Blower power (W) |
| 16 | Q | Heat energy (W) |
| 17 | R | Ideal gas constant ($= 8.314 \text{ J mol}^{-1} \text{K}^{-1}$) |
| 18 | s | Entropy ($\text{J mol}^{-1} \text{K}^{-1}$) |
| 19 | T | Temperature (K) |
| 20 | \bar{T} | Average temperature (K) |
| 21 | ΔT_x | Temperature gradient (K mm^{-1}) |
| 22 | U | Cell voltage (V) |
| 23 | y | Molar fraction |
| 24 | <i>Greek Letters</i> | |
| 25 | γ | Specific heating ratio ($= 1.4$ from [30]) |
| 26 | ε | Heat recovery coefficient |
| 27 | η | Efficiency (%) |
| 28 | μ | Destroyed-to-input exergies ratio |
| 29 | <i>Sub-/Superscripts</i> | |
| 30 | blower | Air blower |
| 31 | ch | Chemical |
| 32 | el | Electrical |
| 33 | en | Energy |
| 34 | ex | Exergy |
| 35 | ef | Effluent |
| 36 | h | Heat stream |
| 37 | i | Species |
| 38 | in | Inlet |
| 39 | ir | Irreversibility |

| | | |
|---|-------|---|
| 1 | insen | Isentropical |
| 2 | m | Material stream |
| 3 | out | Outlet |
| 4 | P | Power |
| 5 | ph | Physical |
| 6 | stack | SOFC stack |
| 7 | th | Thermal |
| 8 | 0 | Reference condition ($T_0 = 298 \text{ K}$, $P_0 = 1.013 \text{ bar}$) |

9 *Acronyms*

| | | |
|----|------|-----------------------|
| 10 | ARR | Anode recycle ratio |
| 11 | BC | Basis case |
| 12 | BoP | Balance of Plant |
| 13 | DF | Designed fuel |
| 14 | SOFC | Solid oxide fuel cell |

15

16 **References**

- 17 (1) Behling, N. H., *Fuel Cells: Current Technology Challenges and Future Research Needs*; Elsevier
18 Science Ltd: New York, 2012.
- 19 (2) Lanzini, A.; Ferrero, D.; Papurello, D.; Santarelli, M., Reporting Degradation from Different Fuel
20 Contaminants in Ni- anode SOFCs. *Fuel Cells*. **2017**.
- 21 (3) Tjønnås, J.; Zenith, F.; Halvorsen, I. J.; Klages, M.; Scholta, J., Control of Reversible Degradation
22 Mechanisms in Fuel Cells: Mitigation of CO contamination. *IFAC-Papers On Line* **2016**, 49, 302.
- 23 (4) Pianko-Oprych, P.; Zinko, T.; Jaworski, Z., A Numerical Investigation of the Thermal Stresses of a
24 Planar Solid Oxide Fuel Cell. *Mater.* **2016**, 9.
- 25 (5) Min, X.; Li, T.; Ming, Y.; Martin, A., Solid oxide fuel cell interconnect design optimization
26 considering the thermal stresses. *Sci. Bull.* **2016**, 61, 1333.
- 27 (6) Recknagle, K. P.; Williford, R. E.; Chick, L. A.; Rector, D. R.; Khaleel, M. A., Three-dimensional
28 thermo-fluid electrochemical modeling of planar SOFC stacks. *J. Power Sources*. **2003**, 113, 109.
- 29 (7) Yakabe, H.; Ogiwara, T.; Hishinuma, M.; Yasuda, I., 3-D model calculation for planar SOFC. *J.*
30 *Power Source.s* **2001**, 102, 144.
- 31 (8) Chiang, L. K.; Liu, H. C.; Shiu, Y. H.; Lee, C. H.; Lee, R. Y., Thermo-electrochemical and thermal
32 stress analysis for an anode-supported SOFC cell. *Renewable Energy* **2008**, 33, 2580.
- 33 (9) Yang, Y.; Wang, G.; Zhang, H.; Xia, W., Computational analysis of thermo-fluid and
34 electrochemical characteristics of MOLB-type SOFC stacks. *J. Power Sources* **2007**, 173, 233.
- 35 (10) Huang, C. M.; Shy, S. S.; Lee, C. H., On flow uniformity in various interconnects and its influence
36 to cell performance of planar SOFC. *J. Power Sources* **2008**, 183, 205.
- 37 (11) Grondin, D.; Deseure, J.; Zahid, M.; Garcia, M. J.; Bultel, Y., Optimization of SOFC interconnect
38 design using Multiphysic computation. In *Computer Aided Chemical Engineering Series 25*; Bertrand,
39 B.; Xavier, J., Eds; Elsevier: Amsterdam, 2008; 841.

- 1 (12) Wang, Y.; Yu, J.; Cao, X., Numerical analysis of optimal performance of planar electrode
2 supported solid oxide fuel cell at various syngas flow rates. *Energy Convers. Manage.* **2014**, 77, 637.
- 3 (13) Riensche, E.; Stimming, U.; Unverzagt, G., Optimization of a 200 kW SOFC cogeneration power
4 plant: Part I: Variation of process parameters. *J. Power Sources* **1998**, 73, 251.
- 5 (14) Amiri, A.; Tang, S.; Vijay, P.; Tadé, M. O., Planar Solid Oxide Fuel Cell Modeling and
6 Optimization Targeting the Stack's Temperature Gradient Minimization. *Ind. Eng. Chem. Res.* **2016**,
7 55, 7446.
- 8 (15) Kumar, R., A critical review on energy, exergy, exergoeconomic and economic (4-E) analysis of
9 thermal power plants. *JESTECH.* **2016**, 20.
- 10 (16) Rosen, M. A.; Dincer, I., Exergy as the confluence of energy, environment and sustainable
11 development. *Exergy Int. J.* **2001**, 1, 3.
- 12 (17) Utlu, Z.; Hepbasli, A., A review on analyzing and evaluating the energy utilization efficiency of
13 countries. *Renew. Sust. Energ. Rev.* **2007**, 11, 1.
- 14 (18) Wongchanapai, S.; Iwai, H.; Saito, M.; Yoshida, H., Selection of suitable operating conditions for
15 planar anode-supported direct-internal-reforming solid-oxide fuel cell. *J. Power Sources* **2012**, 204, 14.
- 16 (19) Braun, R. J.; Klein, S. A.; Reindl, D. T., Evaluation of system configurations for solid oxide fuel
17 cell-based micro-combined heat and power generators in residential applications. *J. Power Sources*
18 **2006**, 158, 1290.
- 19 (20) Duan, L.; Zhang, X.; Yang, Y., *Exergy Analysis of a Novel SOFC Hybrid System with Zero-CO2*
20 *Emission. InTech.* **2011**, 27.
- 21 (21) Bang-Møller, C.; Rokni, M.; Elmegaard, B., Exergy analysis and optimization of a biomass
22 gasification, solid oxide fuel cell and micro gas turbine hybrid system. *Energy* **2011**, 4740.
- 23 (22) Stamatis, A.; Vinni, C.; Bakalis, D.; Tzorbatzoglou, F.; Tsiakaras, P., Exergy Analysis of an
24 Intermediate Temperature Solid Oxide Fuel Cell-Gas Turbine Hybrid System Fed with Ethanol.
25 *Energies* **2012**, 5, 4268.
- 26 (23) Fryda, L.; Panopoulos, K. D.; Karl, J.; Kakaras, E., Exergetic analysis of solid oxide fuel cell and
27 biomass gasification integration with heat pipes. *Energy* **2008**, 33, 292.
- 28 (24) Akkaya, A. V.; Sahin, B.; Huseyin Erdem, H., Exergetic performance coefficient analysis of a
29 simple fuel cell system. *Int. J. Hydrogen Energy* **2007**, 32, 4600.
- 30 (25) Hotz, N.; Senn, S. M.; Poulikakos, D., Exergy analysis of a solid oxide fuel cell micropowerplant.
31 *J. Power Sources* **2006**, 158, 333.
- 32 (26) Calise, F.; Ferruzzi, G.; Vanoli, L., Parametric exergy analysis of a tubular Solid Oxide Fuel Cell
33 (SOFC) stack through finite-volume model. *Appl. Energy* **2009**, 86, 2401.
- 34 (27) Yang, S., Improving a Solid oxide fuel cell system through exergy analysis *Int. J. Exergy* **2016**, 21.
- 35 (28) Amiri, A.; Vijay, P.; Tadé, M. O.; Ahmed, K.; Ingram, G. D.; Pareek, V.; Utikar, R., Solid oxide
36 fuel cell reactor analysis and optimisation through a novel multi-scale modelling strategy. *Comput.*
37 *Chem. Eng.* **2015**, 78, 10.
- 38 (29) Amiri, A.; Vijay, P.; Tadé, M. O.; Ahmed, K.; Ingram, G. D.; Pareek, V.; Utikar, R., Planar SOFC
39 system modelling and simulation including a 3D stack module. *Int. J. Hydrogen Energy* **2016**, 41, 2919.
- 40 (30) Amiri, A.; Tang, S.; Steinberger-Wilckens, R.; Tadé, M. O., Evaluation of fuel diversity in Solid
41 Oxide Fuel Cell system. *Int. J. Hydrogen Energy* **2018**.

- 1 (31) Ii, T. A. A.; Nease, J.; Tucker, D.; Barton, P. I., Energy Conversion with Solid Oxide Fuel Cell
2 Systems: A Review of Concepts and Outlooks for the Short- and Long-Term. *Ind. Eng. Chem. Res.*
3 **2013**, 52, 3089.
- 4 (32) Lin, Z.; Xi, L.; Jiang, J.; Li, S.; Jie, Y.; Jian, L., Dynamic modeling and analysis of a 5-kW solid
5 oxide fuel cell system from the perspectives of cooperative control of thermal safety and high efficiency.
6 *Int. J. Hydrogen Energy* **2015**, 40, 456.
- 7 (33) Liso, V.; Olesen, A. C.; Nielsen, M. P.; Kær, S. K., Performance comparison between partial
8 oxidation and methane steam reforming processes for solid oxide fuel cell (SOFC) micro combined
9 heat and power (CHP) system. *Energy* **2011**, 36, 4216.
- 10 (34) Peters, R.; Deja, R.; Blum, L.; Pennanen, J.; Kiviaho, J.; Hakala, T., Analysis of solid oxide fuel
11 cell system concepts with anode recycling. *International J. Hydrogen Energy* **2013**, 38, 6809.
- 12 (35) Bedringås, K. W.; Ertesvåg, I. S.; Byggstøyl, S.; Magnussen, B. F., Exergy analysis of solid-oxide
13 fuel-cell (SOFC) systems. *Energy* **1997**, 22, 403.
- 14 (36) Nehrir, M.; Wang, C., *Modeling and Control of Fuel Cells: Distributed Generation Applications*;
15 Wiley-IEEE Press: Piscataway 2009.
- 16 (37) Iv, E. J. N.; Sleiti, A. K., Potential of SOFC CHP systems for energy-efficient commercial
17 buildings. *Energy & Buildings* **2013**, 61, 153.
- 18 (38) Pirkandi, J.; Ghassemi, M.; Hamed, M. H.; Mohammadi, R., Electrochemical and thermodynamic
19 modeling of a CHP system using tubular solid oxide fuel cell (SOFC-CHP). *J. Cleaner Prod.* **2012**, 29,
20 151.
- 21 (39) Jiang, J.; Li, X.; Li, J., Modeling and Model-based Analysis of a Solid Oxide Fuel Cell Thermal-
22 Electrical Management System with an Air Bypass Valve. *Electrochim. Acta* **2015**, 177, 250.
- 23 (40) Janardhanan, V. M.; Heuveline, V.; Deutschmann, O., Performance analysis of a SOFC under
24 direct internal reforming conditions. *J. Power Sources* **2007**, 172, 296.
- 25 (41) Kaur, G. *Solid oxide fuel cell components: Interfacial compatibility of SOFC glass seals*; Springer
26 International Publishing: Switzerland, 2015.
- 27 (42) Bejan, A., Tsatsaronis, G., and Moran, M. *Thermal design and optimization*; John Wiley Sons Inc.:
28 New York 1996.
- 29 (43) Nikooyeh, K.; Jeje, A. A.; Hill, J. M., 3D modeling of anode-supported planar SOFC with internal
30 reforming of methane. *J. Power Sources* **2007**, 171, 601.
- 31 (44) Yi, Y.; Rao, A. D.; Brouwer, J.; Samuelsen, G. S., Fuel flexibility study of an integrated 25 kW
32 SOFC reformer system. *J. Power Sources* **2005**, 144, 67.

33

34

35

36

37

38

39

40

1
2
3
4
5
6
7
8
9
10
11
12
13
14
15
16
17
18
19
20
21
22
23

Table 1: Comparison of a number of recent SOFC exergy studies.

| Features | Contributions | | | | | |
|------------|---------------|------|------|---------|---------|-----------|
| | [18] | [19] | [21] | [23-25] | [26-27] | This work |
| I | – | * | * | * | * | * |
| II | – | * | * | – | – | – |
| III | – | * | – | – | * | * |
| IV | – | – | – | – | * | * |
| V | * | * | – | – | – | * |

- Notations:** Considered (*), Not considered (–)
- I.** SOFC exergy evaluation at system level.
 - II.** Exergy evaluation for varying flowsheets.
 - III.** Sensitive analysis of SOFC system based on exergy evaluation.
 - IV.** SOFC system exergy analysis while using detailed stack model in BoP.
 - V.** Operational proposal for thermal management counting the system and stack levels performances metrics.

1
2
3
4
5
6
7
8
9
10
11
12
13
14
15
16
17
18
19
20
21

Table 2: The model parameters for the electrochemical simulation of the SOFC stack and system (BC)

| System operating parameters | Values | |
|--------------------------------------|---|----------------------|
| Fresh fuel composition, molar | 85% CH ₄ + 13% N ₂ + 1.5% H ₂ O + 0.5% C ₂₊ | |
| Fuel flow rate, mol/s | 3.3×10 ⁻⁵ | |
| Fuel inlet temperature, K | 1073 | |
| Cell operating Voltage, V | 0.8 | |
| Stack operating Voltage, V | 3.2 | |
| Operating pressure, bar | 1.0 | |
| Air inlet temperature, K | 1073 | |
| Air to fuel flow rate ratio | 10 | |
| Anode recycling ratio | 0.5 | |
| Pre-reformer temperature, K | 1073 | |
| Fuel cell stack specification | Cathode | Anode |
| Catalyst thickness, m | 2.5×10 ⁻⁴ | 3.0×10 ⁻⁵ |
| Porosity | 0.4 | 0.4 |
| Anodic charge transfer coefficient | 2.0 | 1.4 |
| Cathodic charge transfer coefficient | 1.0 | 0.6 |
| Number of cells within stack | 4 | |
| Cell dimensions, m | 0.1×0.1 | |
| Cell flow pattern | Co-flow of air and fuel | |
| Channel height, m | 7.5×10 ⁻⁴ | |
| Electrolyte thickness, m | 1.0×10 ⁻⁵ | |

1
2
3
4
5
6
7
8
9
10
11
12
13
14
15
16
17
18
19
20
21
22
23
24
25
26
27
28
29
30
31
32
33
34
35
36

Table 3: Variation of system and stack metrics with air flowrate

| $\dot{m}^{air}/\dot{m}_{basis}^{air}$ (-) | \bar{T} (K) | ΔT_x (K/mm) | η_{total}^{ex} (%) | η_{el}^{ex} (%) | η_{th}^{ex} (%) | μ_{ir}^{ex} (%) |
|--|------------------|------------------------|----------------------------|-------------------------|-------------------------|------------------------|
| 0.5 | 1269.6 | 1.93 | 63.3 | 55.7 | 7.6 | 30.4 |
| 1.0 (BC) | 1215.8 | 1.32 | 59.2 | 53.7 | 5.5 | 36.1 |
| 1.5 | 1181.3 | 0.84 | 54.6 | 50.9 | 3.7 | 41.4 |
| 2.0 | 1165.5 | 0.60 | 51.3 | 48.5 | 2.8 | 47.3 |

Table 4: Simulation results for the system and stack behavior deploying various oxygen concentrations in fresh air.

| y_{O_2} (-) | \bar{T} (K) | ΔT_x (K/mm) | η_{total}^{ex} (%) | η_{el}^{ex} (%) | η_{th}^{ex} (%) | μ_{ir}^{ex} (%) |
|------------------|------------------|------------------------|----------------------------|-------------------------|-------------------------|------------------------|
| 0.21 (BC) | 1215.8 | 1.32 | 59.2 | 53.7 | 5.5 | 36.1 |
| 0.25 | 1218.4 | 1.33 | 59.6 | 54.5 | 5.1 | 35.7 |
| 0.30 | 1219.6 | 1.34 | 60.0 | 55.3 | 4.7 | 35.4 |
| 0.35 | 1220.1 | 1.35 | 60.4 | 55.9 | 4.6 | 34.9 |
| 0.40 | 1221.5 | 1.36 | 60.9 | 56.4 | 4.5 | 34.6 |

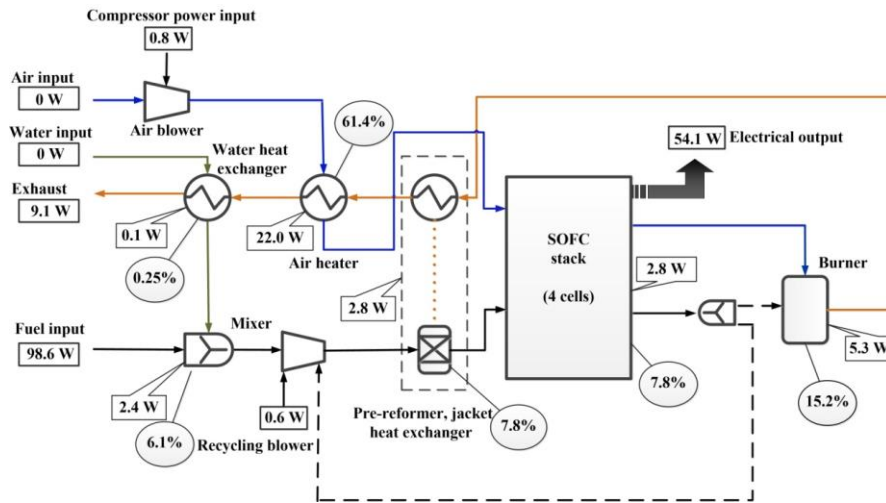
1
2
3
4
5
6
7
8
9
10
11
12
13
14
15
16
17
18
19
20
21

Table 5: Simulation results for the system thermal behaviour against ARR.

| ARR (-) | \bar{T} (K) | ΔT_x (K/mm) | η_{total}^{ex} (%) | η_{el}^{ex} (%) | η_{th}^{ex} (%) | μ_{ir}^{ex} (%) |
|------------|------------------|------------------------|----------------------------|-------------------------|-------------------------|------------------------|
| 0.1 | 1208.0 | 1.07 | 55.6 | 49.3 | 6.2 | 38.7 |
| 0.3 | 1213.1 | 1.21 | 57.3 | 51.4 | 5.9 | 37.5 |
| 0.5 (BC) | 1215.8 | 1.32 | 59.2 | 53.7 | 5.5 | 36.1 |
| 0.7 | 1221.1 | 1.39 | 60.0 | 54.7 | 5.3 | 35.2 |

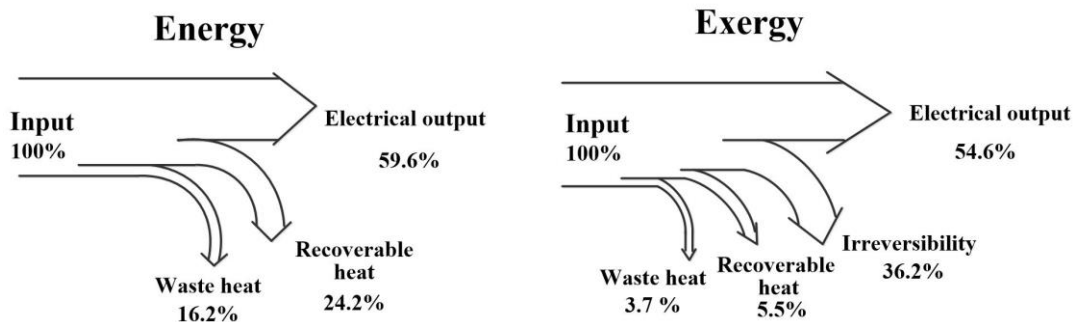
Table 6: Simulation results for the system thermal behaviour operating on different fuels.

| Fuel | \bar{T} (K) | ΔT_x (K/ mm) | η_{total}^{ex} (%) | η_{el}^{ex} (%) | η_{th}^{ex} (%) | μ_{ir}^{ex} (%) |
|---|--|----------------------------|----------------------------|-------------------------|-------------------------|------------------------|
| BC | 1215.8 | 1.32 | 59.2 | 53.7 | 5.5 | 36.1 |
| Designed fuel (I) | 1207.0 | 1.25 | 52.0 | 42.9 | 10.1 | 38.8 |
| Designed fuel (II) | 1201.0 | 1.17 | 47.2 | 30.8 | 16.5 | 40.5 |
| Syngas | 1194.5 | 1.06 | 44.0 | 23.8 | 20.2 | 41.3 |
| Fuel | Composition | | Flowrate (mol/s) | | | |
| BC | CH ₄ 85%, N ₂ 13% H ₂ O 1.5 %, C ₂₊ 0.5% | | 3.3×10 ⁻⁵ | | | |
| Syngas ⁴⁴ | 36% H ₂ + 46% CO + 18 % CO ₂ | | 1.1×10 ⁻⁴ | | | |
| Designed fuel (I) | 70% Basis fuel + 30% Syngas | | 5.6×10 ⁻⁵ | | | |
| Designed fuel (II) | 30% Basis fuel + 70% Syngas | | 8.7×10 ⁻⁵ | | | |
| $Ex_{Design\ Fuel} = y_{BC} \times Ex_{BC} + y_{Syngas} \times Ex_{Syngas}$ | | | | | | |



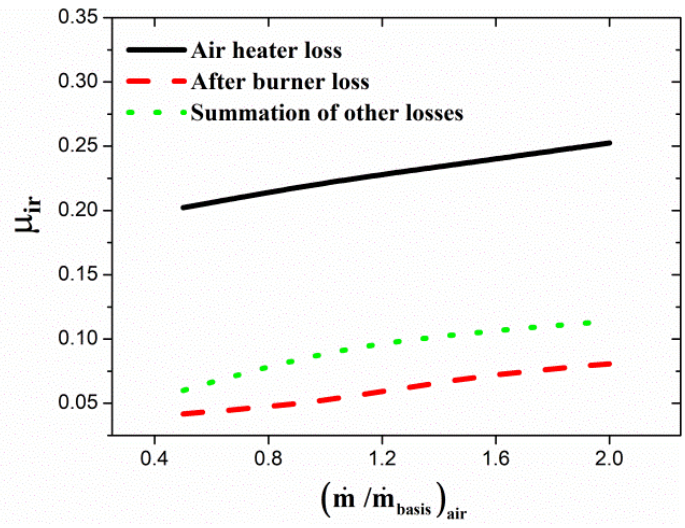
1
2
3
4
5
6
7
8
9

Figure 1: Process layout for a SOFC system showing the indicative exergy results for the basis case simulation including the sub-process exergy loss (rectangular boxes with arrow), exergy loss to the input exergy into the system ratio (oval boxes), and system input and output exergies (rectangular boxes without arrow).



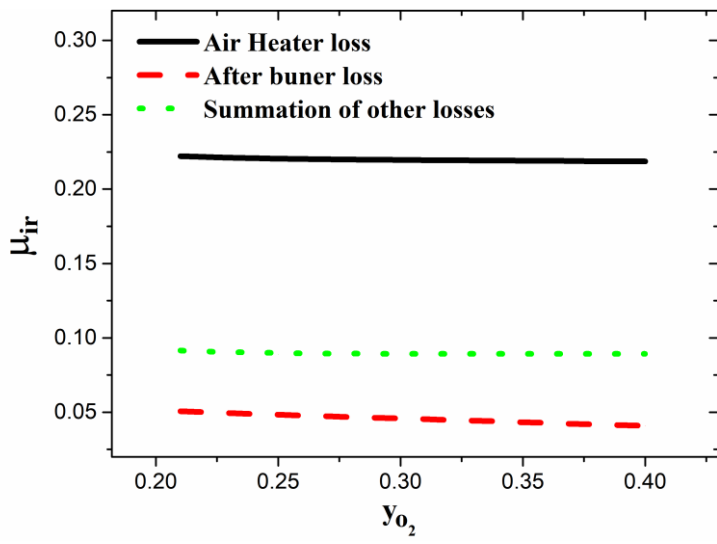
10
11
12
13
14
15
16
17
18

Figure 2: The plant analysis based on energy and exergy principles.



1
2
3
4

Figure 3: Ratio of the exergy losses to the total exergy input for different air flow rates.



5
6
7
8
9
10
11
12
13
14
15

Figure 4: Ratio of the exergy losses to the total exergy input for different oxygen concentrations used in cathode gas.

1
2
3

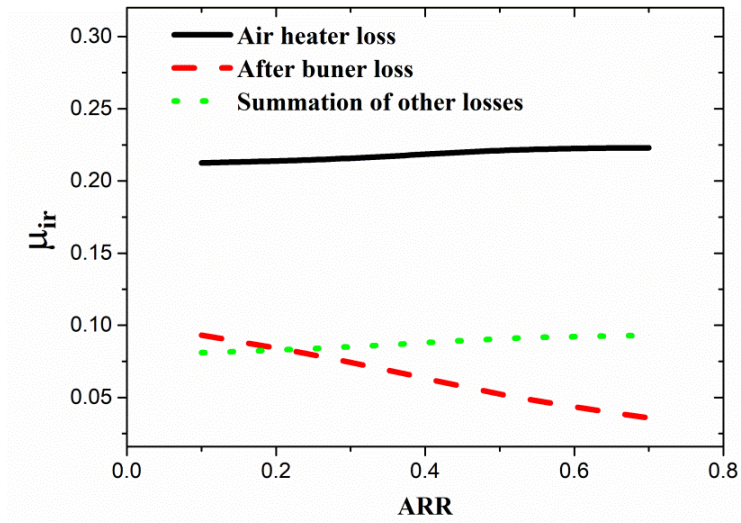


Figure 5: Effect of ARR on BoP units' exergy loss ratio.

4
5
6
7

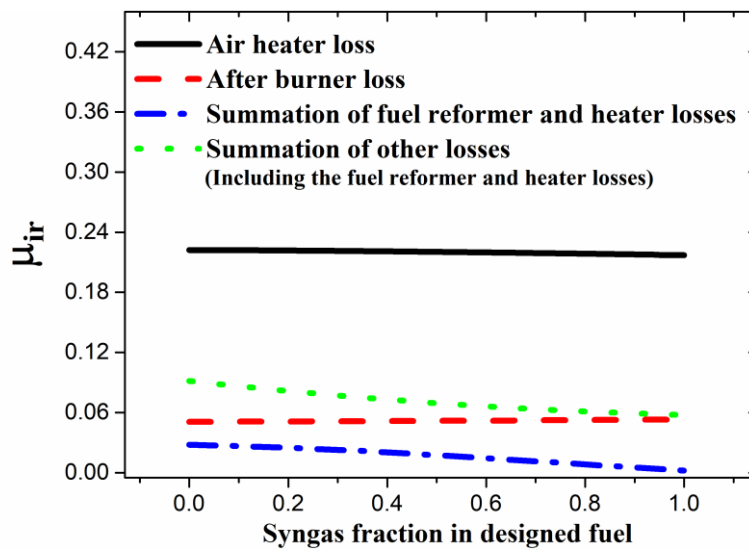
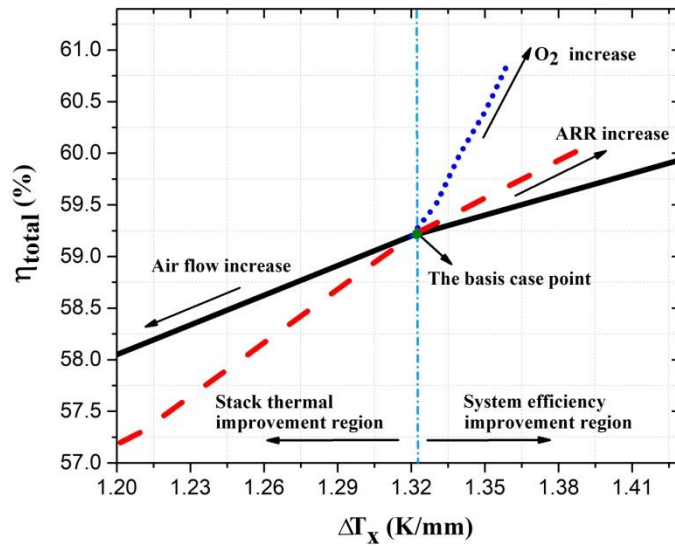


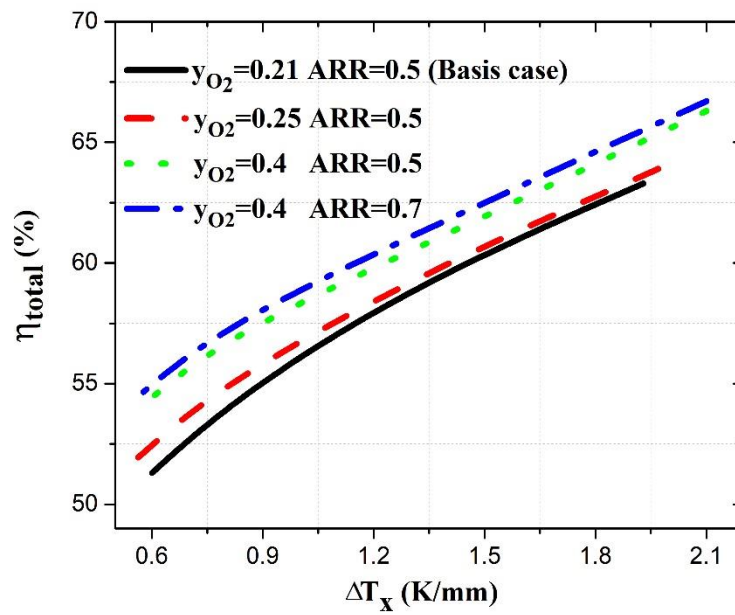
Figure 6: Ratio of the exergy loss to the total exergy input for different fuel compositions used in the system.

8
9
10
11
12
13



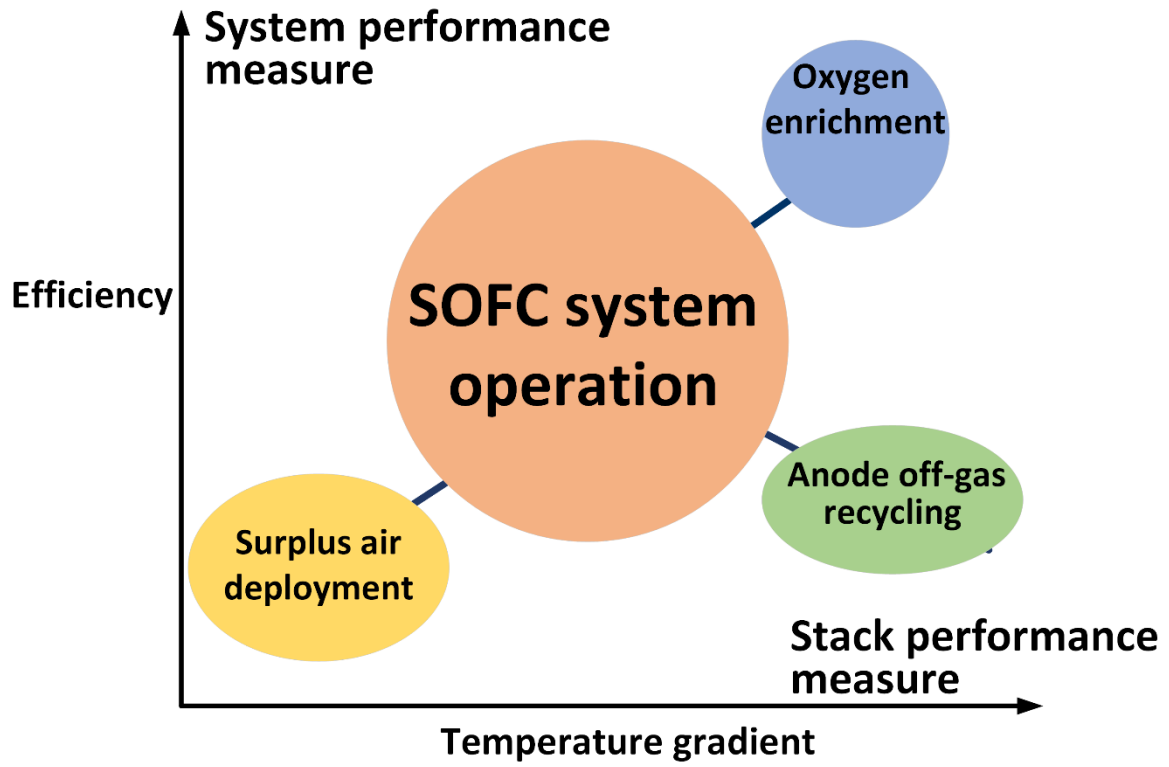
1
2
3
4

Figure 7: System efficiency against the stack temperature gradient for individual operational strategies.



5
6
7
8
9
10
11
12
13

Figure 8: System exergy-based efficiency against the stack thermal gradient for coolant air flowrates varying from 0.5 to 2 times of the basis air flow, combined with ARR and y_{O_2} impacts.



- 1
- 2
- 3
- 4

For Table of Contents Only